

Subcutaneous Adipose Tissue Macrophage Infiltration Is Associated With Hepatic and Visceral Fat Deposition, Hyperinsulinemia, and Stimulation of NF- κ B Stress Pathway

Kim-Anne Lê,¹ Swapna Mahurkar,¹ Tanya L. Alderete,¹ Rebecca E. Hasson,¹ Tanja C. Adam,¹ Joon Sung Kim,^{1,2} Elizabeth Beale,³ Chen Xie,⁴ Andrew S. Greenberg,⁴ Hooman Allayee,¹ and Michael I. Goran¹

OBJECTIVE—To examine in obese young adults the influence of ethnicity and subcutaneous adipose tissue (SAT) inflammation on hepatic fat fraction (HFF), visceral adipose tissue (VAT) deposition, insulin sensitivity (SI), β -cell function, and SAT gene expression.

RESEARCH DESIGN AND METHODS—SAT biopsies were obtained from 36 obese young adults (20 Hispanics, 16 African Americans) to measure crown-like structures (CLS), reflecting SAT inflammation. SAT, VAT, and HFF were measured by magnetic resonance imaging, and SI and β -cell function (disposition index [DI]) were measured by intravenous glucose tolerance test. SAT gene expression was assessed using Illumina microarrays.

RESULTS—Participants with CLS in SAT ($n = 16$) were similar to those without CLS in terms of ethnicity, sex, and total body fat. Individuals with CLS had greater VAT (3.7 ± 1.3 vs. 2.6 ± 1.6 L; $P = 0.04$), HFF (9.9 ± 7.3 vs. $5.8 \pm 4.4\%$; $P = 0.03$), tumor necrosis factor- α (20.8 ± 4.8 vs. 16.2 ± 5.8 pg/mL; $P = 0.01$), fasting insulin (20.9 ± 10.6 vs. 9.7 ± 6.6 mU/mL; $P < 0.001$) and glucose (94.4 ± 9.3 vs. 86.8 ± 5.3 mg/dL; $P = 0.005$), and lower DI ($1,559 \pm 984$ vs. $2,024 \pm 829 \times 10^{-4} \text{ min}^{-1}$; $P = 0.03$). Individuals with CLS in SAT exhibited upregulation of matrix metalloproteinase-9 and monocyte antigen CD14 genes, as well as several other genes belonging to the nuclear factor- κ B (NF- κ B) stress pathway.

CONCLUSIONS—Adipose tissue inflammation was equally distributed between sexes and ethnicities. It was associated with partitioning of fat toward VAT and the liver and altered β -cell function, independent of total adiposity. Several genes belonging to the NF- κ B stress pathway were upregulated, suggesting stimulation of proinflammatory mediators. *Diabetes* 60:2802–2809, 2011

Adipose tissue inflammation is now recognized as an important mediating link that may help explain the relationship between obesity and several metabolic abnormalities, including insulin resistance (1,2), liver fat accumulation (1,2), and vascular

dysfunction (3). This association, however, is not consistent across obese individuals. For example, despite a similar degree of obesity, some obese individuals develop insulin resistance, type 2 diabetes, and nonalcoholic fatty liver disease, whereas others remain protected. This has led to the description of metabolically healthy obese patients (4) who display low hepatic fat content and high insulin sensitivity (SI) together with a favorable inflammatory profile (5). One factor that may explain differences in metabolic risk between individuals with the same degree of body fat is adipose tissue inflammation.

Adipose tissue has long been considered as an inactive tissue, in which its presumed primary role was to store energy excess as triglycerides (TG). It is now widely accepted that adipose tissue acts as an endocrine organ as well through secretion of various adipokines and cytokines and plays a role in regulation of metabolic pathways (6). In obese individuals, excessive storage of free fatty acids (FFA) as TGs may lead to subcutaneous adipose tissue (SAT) dysfunction, resulting in impaired TG storage and possibly diversion of FFA to other tissues, such as the liver or the visceral compartment (7). Such a condition has been associated with high adipose tissue inflammation, characterized by higher secretion of proinflammatory cytokines and macrophage recruitment. Previous research has demonstrated that in adipose tissue from obese mice and humans, such macrophages aggregate around dead adipocytes, forming characteristic ring patterns referred to as crown-like structures (CLS) (8). Furthermore, the macrophages within CLS have been shown to be proinflammatory, and their presence is associated with insulin resistance (9,10).

Hispanics are more prone to an ectopic fat pattern, such as visceral and liver fat accumulation (11), when compared with African Americans; this may be driven partly by impaired SAT storage function and associated with adipose macrophage infiltration (12). Conversely, African Americans are similarly prone to obesity but appear protected against visceral and hepatic fat accumulation.

The purpose of this study, therefore, was to investigate the effect of adipose tissue inflammation on visceral and hepatic fat deposition, SI, and adipose tissue gene expression in two different ethnic groups. We hypothesized that individual differences in adipose tissue inflammation, reflected by the presence of CLS, may explain metabolic abnormalities of obesity, such as hepatic fat deposition and insulin resistance. We therefore recruited participants of Hispanic and African American ethnicity, who are obese and at high risk for type 2 diabetes but

From the ¹Department of Preventive Medicine, Childhood Obesity Research Center, University of Southern California, Los Angeles, California; the ²Department of Pediatrics, Ulsan University Hospital, University of Ulsan College of Medicine, Ulsan, South Korea; the ³Department of Internal Medicine/Division of Endocrinology and Diabetes, Keck School of Medicine, University of Southern California, Los Angeles, California; and the ⁴Jean Mayer USDA Human Nutrition Research Center on Aging at Tufts University, Tufts University School of Medicine, Boston, Massachusetts.

Corresponding author: Michael I. Goran, goran@usc.edu.

Received 7 September 2010 and accepted 26 May 2011.

DOI: 10.2337/db10-1263. Clinical trial reg. no. NCT00697580, clinicaltrials.gov.

© 2011 by the American Diabetes Association. Readers may use this article as long as the work is properly cited, the use is educational and not for profit, and the work is not altered. See <http://creativecommons.org/licenses/by-nc-nd/3.0/> for details.

show very distinct fat repartition patterns, and investigated whether histological and gene expression differences in adipose tissue contribute to poor metabolic outcomes, such as higher liver fat and insulin resistance.

RESEARCH DESIGN AND METHODS

Study participants. This cross-sectional analysis includes 36 obese (BMI ≥ 30 kg/m²) African American (7 men, 9 women) or Hispanic participants (9 men, 11 women) aged 18–25 years. Participants were excluded if they had taken medications known to affect body composition, been diagnosed with any major illness since birth, or had any diagnostic criteria for diabetes. Written informed consent and assent were received from all participants. This study was approved by the Institutional Review Board of the Keck School of Medicine, University of Southern California.

Fat quantification. Whole-body fat was measured by dual-energy X-ray absorptiometry using a Hologic QDR 4500 W (Hologic, Bedford, MA). Abdominal magnetic resonance imaging data were obtained by the Dixon method, with a sensitive three-point chemical-shift fat-water separation method using a 1.5 Tesla Siemens Symphony Maestro whole-body scanner (Siemens AG, Erlangen, Germany) with Numaris 4 software. A two-dimensional multislice breath-hold protocol previously reported by Hussain et al. (13) was adopted to obtain 19 axial images across the abdomen from the dome of the liver to the L2-L3 vertebrae. The slice thickness was 10 mm with no interslice gaps. The fat-only dataset was used in the subsequent quantification of SAT volume and visceral adipose tissue (VAT) volume, whereas the fat fraction dataset was used to assess percent hepatic fat content (hepatic fat fraction [HFF]). A commercially available image segmentation and quantification software

(SliceOmatic; Tomovision, Inc.) was used. SAT and VAT volumes were computed across all 19 image slices in each participant. HFF was computed as the mean fat fraction of all imaging slices within which the liver was present.

SAT collection. Abdominal SAT biopsies were performed lateral to the umbilicus in the skin crease below the abdominal pannus in the lower abdomen using standard sterile techniques. The region was locally anesthetized with 2 mL of 2% lidocaine. Through a 0.5-cm skin incision, SAT was collected with a disposable 0.5-cm diameter biopsy punch using three passes. All tissue samples were stored in formalin or promptly frozen in liquid nitrogen (LN2) and stored at -80°C .

Adipose tissue immunohistochemistry. Infiltration of macrophage cell populations into adipose tissue was characterized using cell-specific stains against CD68, an established cell surface marker for macrophages (predilute antibodies from DakoCytomation Corporation). In brief, 5- μm -thick adipose tissue sections were fixed and loaded onto a Biotex I-6000 machine for incubation with primary antibodies. Multilink biotinylated secondary antibody was then allowed to react for 30 min at room temperature. Slides were then washed with PBS and placed in diaminobenzidine solution and microscopically examined for a positive reaction and counterstained with hematoxylin. All samples were evaluated in a blinded fashion by the pathologist for the presence (+) or absence (–) of macrophage CLS, indicating the presence of dead adipocytes (8). Tissue sections were observed with a Nikon Eclipse E800 light microscope using a $\times 20$ objective, and digital images were captured with a DXM 1200 camera. CLS density (CLS per 400 adipocytes) was determined using a drawing tablet and the Nikon Lucia IMAGE version 4.61 morphometric program. Four representative tissue sections in each sample were observed, and participants were dichotomously categorized as being CLS+ if distinct adipose tissue macrophage clusters were present in any examined high-power

TABLE 1

Anthropometric, body composition, SI, and plasma parameters stratified by adipose tissue inflammatory status

	CLS–	CLS+	P value
<i>n</i>	20	16	
Number of CLS (per 400 adipocyte)	0 \pm 0	12.9 \pm 17.9	0.002
Age (years)	21.6 \pm 2.2	21.1 \pm 2.4	NS
Sex (men/women)	8/12	8/8	NS
Ethnicity (Hispanic/African American)	10/10	10/6	NS
Body composition			
BMI (kg/m ²)	35.1 \pm 3.3	36.3 \pm 4.1	NS
Total fat (%)	37.7 \pm 7.4	37.3 \pm 6.3	NS
SAT (L)	16.0 \pm 4.9	17.3 \pm 3.9	NS
VAT (L)	2.6 \pm 1.6	3.7 \pm 1.3	0.04
HFF (%)	5.8 \pm 4.4	9.9 \pm 7.3	0.03
SI			
Fasting glucose (mg/dL)	86.8 \pm 5.3	94.4 \pm 9.3	0.005
Fasting insulin (mU/mL)	9.7 \pm 6.6	20.9 \pm 10.6	<0.001
HOMA-IR	2.0 \pm 1.4	4.4 \pm 2.2	<0.001
HOMA- β -cell	191.4 \pm 125.4	399 \pm 301	0.01
Acute insulin response (mU/mL \times 10 min)	1,320 \pm 912	1,116 \pm 796	NS
SI ($\times 10^{-4}$ min ⁻¹ /mU/mL)	1.9 \pm 0.7	1.3 \pm 0.9	NS
DI ($\times 10^{-4}$ min ⁻¹)	2,024 \pm 829	1,559 \pm 984	0.03
Lipid metabolism			
FFAs (mmol/L)	0.87 \pm 0.19	0.83 \pm 0.15	NS
TGs (mg/dL)	113 \pm 59	102 \pm 48	NS
Cholesterol (mg/dL)			
Total	155 \pm 31	158 \pm 35	NS
LDL	81 \pm 26	94 \pm 39	NS
HDL	50 \pm 11	43 \pm 13	0.09
Inflammation			
MCP-1 (pg/mL)	349 \pm 182	379 \pm 97	NS
IL-8 (pg/mL)	9.7 \pm 3.3	11.4 \pm 3.2	NS
TNF- α (pg/mL)	16.2 \pm 5.8	20.8 \pm 4.8	0.01
HGF (ng/mL)	2.1 \pm 0.8	2.1 \pm 0.8	NS
PAI-1 (ng/mL)	104 \pm 44	121 \pm 43	NS
hs-CRP (mg/L)	7.7 \pm 16.2	6.7 \pm 8.3	NS
Leptin (ng/mL)	45 \pm 22	51 \pm 28	NS
Adiponectin (mg/mL)	17 \pm 6	14 \pm 5	NS

Data are means \pm SD. HGF, hepatocyte growth factor; hs-CRP, high-sensitivity C-reactive protein; NS, not significant; PAI-1, plasminogen activator inhibitor 1.

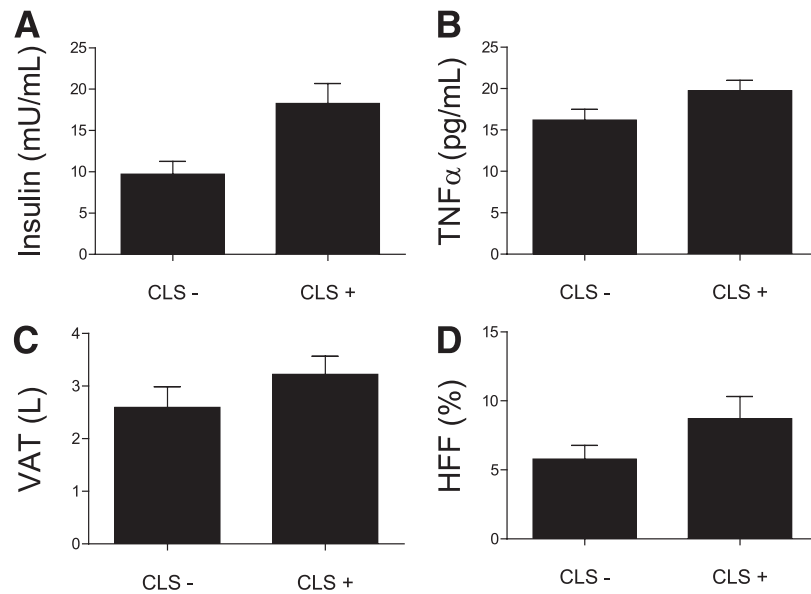


FIG. 1. Fasting insulin (A), TNF- α concentrations (B), VAT volume (C), and HFF (D) stratified by adipose tissue CLS status. All P values < 0.05.

field or CLS- if clusters were completely absent in all histological fields for a given participant. To further characterize macrophage type, we performed CD11c immunoreactivity in six CLS+ (four Hispanics, two African Americans) and four CLS- participants (three Hispanics, one African American) using a mouse monoclonal antibody against human CD11c, a specific cell surface marker for type 1 macrophages (Novacastra Mouse Monoclonal Antibody CD11c [Clone 5D11]).

Adipose tissue microarray analysis. Total RNA was isolated from adipose tissue biopsies using RNeasy Mini kits (Qiagen, Valencia, CA). Biotinylated RNA for hybridization with the Illumina arrays was amplified using the TotalPrep RNA Amplification Kit. Global gene expression was determined for each sample using an Illumina (San Diego, CA) HumanHT-12 v3 expression bead chip through a service provided by the Southern California Genotyping Consortium (<http://scgc.genetics.ucla.edu/>). Quality control was performed and fulfilled the criteria for array hybridization suggested by the Tumor Analysis Best Practices Working Group (14). Data analysis was performed using Genome studio and Partek Inc. (St. Louis, MO). Background corrected and quantile normalized signal intensity values were exported to Partek. Array data have been submitted to the Gene Expression Omnibus (accession: GSE23506). A fold change of 1.3 was used as a criterion for inclusion of genes in functional annotation and pathway analysis. Our study was 70% powered to detect a fold change of 1.3 (<http://bioinformatics.mdanderson.org/MicroarraySampleSize/MicroarraySampleSize.aspx>).

RT-PCR. Genes of interest were validated using quantitative RT-PCR. Reverse transcription was performed with 0.5 μ g of total RNA and random hexamer primers (Applied Biosystems, Foster City, CA). Inventoried and validated TaqMan probes were used. RT-PCR amplification was performed using an ABI HT7900 instrument (Applied Biosystems). All values are expressed as the average relative expression normalized to GUS-B endogenous control subjects.

SI and intravenous glucose tolerance test. An insulin-modified frequently sampled intravenous glucose tolerance test (IVGTT) (15) was performed after an overnight fast. Upon arrival, a catheter was inserted into both arms at the antecubital level. At time 0, glucose (25% dextrose, 0.3 g/kg body wt) was administered intravenously. Insulin (0.02 units/kg body wt, Humulin R [regular insulin for human injection]; Eli Lilly, Indianapolis, IN) was injected intravenously at 20 min. Blood samples of glucose and insulin were collected at time points -15, -5, 2, 4, 8, 19, 22, 30, 40, 50, 70, 100, and 180 min and of FFA, TG, cholesterol, and cytokines at time -15. Glucose and insulin values obtained from the IVGTT were entered into the MINMOD Millennium 2003 computer program (version 5.16, Bergman, USC) to determine SI, glucose effectiveness, acute insulin response (AIR), and disposition index (DI) (15). Homeostasis model assessment-insulin resistance (HOMA-IR) was calculated according to the following formula: fasting insulin [mU/mL] \times fasting glucose [mmol/L]/22.5, while HOMA- β -cell = 20 \times fasting insulin [mU/mL]/fasting glucose [mmol/L] - 3.5.

Blood analysis. Blood samples from all time points taken during the IVGTT were centrifuged immediately for 10 min at 2,500 revolutions per minute at 8–10°C and

frozen at -70°C until analysis. Glucose was assayed in duplicate on a Yellow Springs Instrument 2700 Analyzer (Yellow Springs, OH) using the glucose oxidase method. Insulin was assayed in duplicate using a specific human insulin ELISA kit from Linco (St. Charles, MO), and FFA were quantified using a colorimetric kit (NEFA-HR(2); Wako Diagnostics, Richmond, VA). TGs and total, LDL, and HDL cholesterol were measured using the Kodak Ektachem DT slide assay. Circulating inflammatory mediators including plasminogen activator inhibitor 1, monocyte chemoattractant protein 1 (MCP-1), interleukin-8 (IL-8), tumor necrosis factor- α (TNF- α), and hepatocyte growth factor were measured in batch using multiplex Luminex assays (Linco Research). High-sensitivity C-reactive protein was measured chemically using ADVIA 1800 Chemistry System (Siemens Healthcare Diagnostics, Deerfield, IL).

Statistical methods. All data are means \pm SD, unless otherwise specified. Statistical analyses were performed using STATA 11.0 (Stata Corporation, College Station, TX). P values < 0.05 were considered statistically significant. Values for high-sensitivity C-reactive protein were log-transformed to reach a normal distribution. Unadjusted comparisons for parameters between adipose inflammatory status were done using Student t tests. Adjustments of comparisons for sex, ethnicity, total fat, and VAT were performed using ANCOVA when appropriate. Because of the large SDs of HOMA- β -cell, SI, AIR, and DI, these parameters were tested using the nonparametric Wilcoxon signed-rank test. χ^2 Tests were performed to assess the effect of ethnicity and sex on inflammatory status. Correlation analyses were done using Pearson correlation tests. Differentially expressed genes were determined using one-way ANOVA and exported to Ingenuity pathway analysis 8.6 (Ingenuity Systems, Redwood City, CA).

RESULTS

Clinical and histological data. A total of 36 obese participants with an average BMI of 35.6 ± 3.9 kg/m² completed the study (mean age 21.2 ± 2.3 years; 55% Hispanics, 55% women). We first carried out histological analyses of adipose biopsies to determine the presence of aggregated macrophages as CLS. Mean section area was 14.0 ± 5.1 mm²; 16 participants showed presence of CLS (CLS+), whereas there were no signs of CLS in the remaining 20 participants (CLS-). In the CLS+ participants, the mean number of CLS per 400 adipocytes was 12.9 ± 17.9 , with a median of 5.4 and an interquartile range of 2.4–14.2. The characteristics of the participants, stratified by CLS status, are shown in Table 1. Of note, CLS+ participants were equally distributed among men and women as well as Hispanics and African Americans (χ^2 tests: $P > 0.05$), even after adjusting for total fat and VAT.

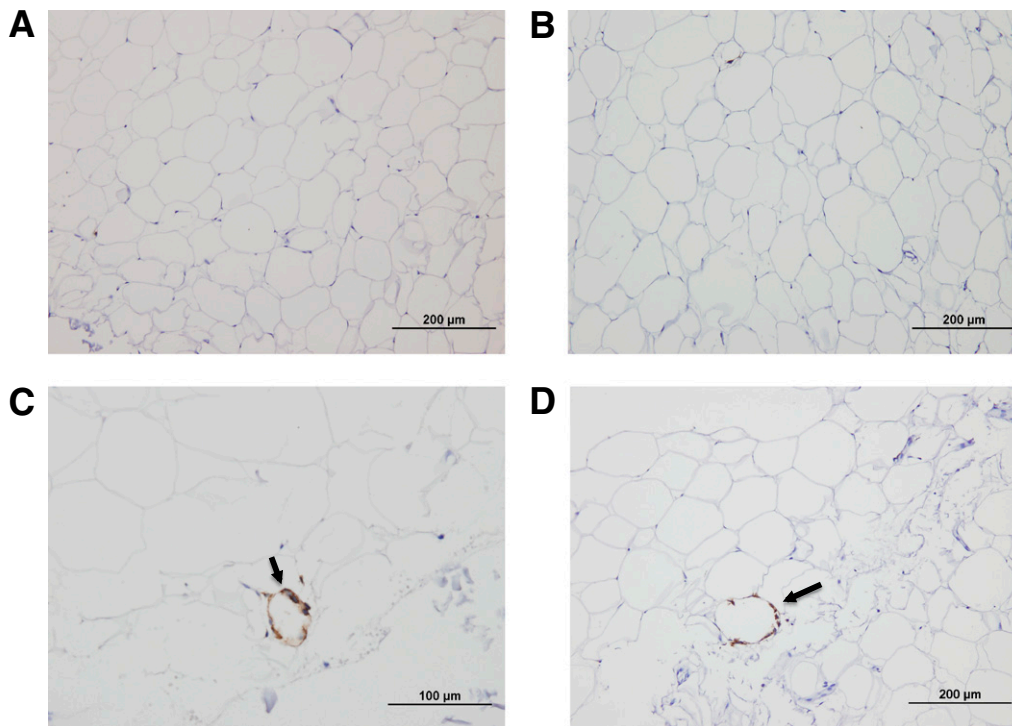


FIG. 2. Identification of CD11c⁺ macrophages (arrows) in CLS⁻ (A and B) and CLS⁺ (C and D) individuals. Note the presence of CD11c⁺ immunoreactivity (brown staining) only in subjects with CLS. (A high-quality digital representation of this figure is available in the online issue.)

This suggests that major differences with respect to the presence of CLS are not driven by sex or ethnicity in our study population. In the whole group, CLS⁺ individuals had increased VAT (3.7 ± 1.3 vs. 2.6 ± 1.6 L; $P = 0.04$), HFF (9.9 ± 7.3 vs. $5.8 \pm 4.4\%$; $P = 0.03$), fasting TNF- α (20.8 ± 4.8 vs. 16.2 ± 5.8 pg/mL; $P = 0.01$), and insulin concentrations (20.8 ± 2.6 vs. 9.7 ± 6.5 mU/mL; $P = 0.0007$), independent of sex, ethnicity, total fat, and visceral fat volume (Fig. 1). Markers of insulin resistance, including fasting glucose, fasting insulin, HOMA-IR, and HOMA- β , were also significantly higher in the CLS⁺ group, compared with the CLS⁻, and these comparisons remained significant after adjusting for covariates. DI, reflecting β -cell function, was significantly lower in the CLS⁺ group ($1,559 \pm 984$ vs. $2,024 \pm 829 \times 10^{-4} \text{ min}^{-1}$; $P = 0.03$), whereas SI, glucose effectiveness, and AIR were not significantly different (Table 1). HDL cholesterol concentrations tended to be lower in CLS⁺ participants ($P = 0.09$), but there were no differences in fasting TGs and total and LDL cholesterol concentrations. In a subset of participants, we performed further immunohistochemical studies to examine the presence of CD11c⁺ immunoreactivity, to detect the presence of dendritic cells. Of the six participants with CLS⁺, four of them showed positive CD11c immunoreactivity staining, whereas it was completely absent in all four CLS⁻ participants (Fig. 2). CD11c⁺ cells are a subclass of macrophages, called dendritic cells, which have been demonstrated to be proinflammatory and linked to systemic insulin resistance (10,16).

We then investigated whether presence of CLS translated into the same phenotypes between Hispanics and African Americans. When analyses were stratified by ethnicity, presence of CLS was specifically associated with higher VAT (2.8 ± 0.9 vs. 1.6 ± 0.9 L; $P = 0.02$) and glucose (100.1 ± 8.6 vs. 84.4 ± 5.6 mg/dL; $P < 0.001$) in African Americans. In

Hispanics, CLS was associated with higher TNF- α (22.6 ± 3.8 vs. 16.5 ± 5.8 pg/mL; $P = 0.01$) and a trend for lower SI (1.6 ± 0.4 vs. $2.1 \pm 0.2 \times 10^{-4} \text{ min}^{-1}/\text{mU/mL}$; $P = 0.06$).

Adipose tissue gene expression analysis. In the same participants, we subsequently assessed gene expression in SAT biopsies. Of the 23,000 known annotated genes analyzed on the Illumina Human HT-12 chip, 375 genes (~2%) were differentially expressed between the CLS⁺ and CLS⁻ groups based on a detection P value < 0.05 . Table 2 shows the top 15 differentially up- and downregulated genes in CLS⁺ compared with CLS⁻ individuals. Based on Gene Ontology descriptions, molecules involved in inflammatory disease, such as matrix metalloproteinase-9 (*MMP9*; fold change: +4.8; $P = 0.0004$), interferon γ -inducible protein 30 (fold change: +2.2; $P = 0.003$), and IL-1 receptor antagonist (fold change: +2.0; $P = 0.03$), were among the most upregulated genes in CLS⁺ subjects compared with CLS⁻ individuals. Genes involved in response to inflammation were also upregulated, including lipopolysaccharide binding protein (fold change: +2.0; $P = 0.004$), TNF receptor superfamily, member 11b (fold change: +1.4; $P = 0.01$), *MCP-1* (fold change: +1.6; $P = 0.02$), and monocyte antigen *CD14* (fold change: +1.5; $P = 0.01$). By comparison, insulin receptor substrate (*IRS-1*) (fold change: -1.6; $P = 0.02$) and *IRS-2* (fold change: -1.5; $P = 0.01$), which play central roles in the insulin signaling cascade, were downregulated in CLS⁺ individuals. Importantly, the differential expression of these inflammatory and insulin signaling genes was observed in both Hispanics and African Americans. On the basis of their relevance to inflammatory pathways we selected the following genes for RT-PCR validation: *CD14*, *MMP9*, suppressor of cytokine signaling 3, and *IRS-1*. In agreement with our hypothesis and the microarrays results, CLS⁺ individuals showed upregulation of *CD14* (1.7 ± 0.9 vs. 0.9 ± 0.3 ; $P = 0.02$) and *MMP9* (1.3 ± 1.1 vs. 0.3 ± 0.2 ;

TABLE 2
Top 15 up- and downregulated genes in CLS+ compared with CLS- individuals

Upregulated in CLS+ individuals				Downregulated in CLS+ individuals			
Unigene official gene symbol	Gene name	P value	Fold change	Unigene official gene symbol	Gene name	P value	Fold change
<i>MMP9</i>	matrix metalloproteinase 9	0.0004	+4.8	<i>KRT15</i>	keratin 15	0.04	-2.2
<i>SPP1</i>	secreted phosphoprotein 1	0.01	+3.2	<i>CIDEA</i>	cell death-inducing DFFA-like effector a	0.04	-1.9
<i>SLC2A5</i>	solute carrier family 2 (facilitated glucose/fructose transporter), member 5	0.0001	+2.7	<i>COBL</i>	cordon-bleu homolog (mouse)	0.01	-1.9
<i>PLA2G7</i>	platelet-activating factor acetylhydrolase, plasma	0.005	+2.6	<i>COL6A6</i>	collagen, type VI, α -6	0.004	-1.8
<i>IFI30</i>	interferon, γ -inducible protein 30	0.003	+2.2	<i>CEACAM6</i>	carcinoembryonic antigen-related cell adhesion molecule 6	0.04	-1.8
<i>PLA2G2A</i>	phospholipase A2, group IIA	0.003	+2.1	<i>S100P</i>	S100 calcium binding protein P	0.02	-1.6
<i>LBP</i>	lipopolysaccharide binding protein	0.004	+2.1	<i>GSDMB</i>	gasdermin B	0.02	-1.6
<i>ITGAX</i>	integrin, α -X	0.006	+2.0	<i>GISH</i>	cytokine inducible SH2-containing protein	0.02	-1.6
<i>IL1RN</i>	IL-1 receptor antagonist	0.03	+2.0	<i>ALDH3B2</i>	aldehyde dehydrogenase 3 family, member B2	0.04	-1.6
<i>CLIC6</i>	chloride intracellular channel 6	0.03	+2.0	<i>ADH1A</i>	alcohol dehydrogenase 1A (class I), α -polypeptide	0.006	-1.6
<i>CHI3L2</i>	chitinase 3-like 2	0.001	+2.0	<i>IRS1</i>	insulin receptor substrate 1	0.02	-1.6
<i>HMOX1</i>	heme oxygenase 1	0.0001	+2.0	<i>FHOD3</i>	formin homology 2 domain containing 3	0.02	-1.6
<i>ACP5</i>	acid phosphatase 5	0.007	+2.0	<i>IRS2</i>	insulin receptor substrate 2	0.01	-1.5
<i>PRND</i>	prion protein 2	0.005	+1.9	<i>RAP1GAP</i>	RAP1 GTPase activating protein	0.03	-1.5
<i>HP</i>	haptoglobin	0.009	+1.8	<i>ADH1B</i>	alcohol dehydrogenase 1B (class I), β -polypeptide	0.02	-1.5

Positive fold change, upregulated in individuals with CLS (CLS+); negative fold change, downregulated in individuals with CLS (CLS-).

$P = 0.01$) compared with CLS- individuals. The suppressor of cytokine signaling 3 was upregulated (1.5 ± 1.9 vs. 0.8 ± 0.5 ; $P = 0.2$) and *IRS1* was downregulated in CLS+ individuals (1.0 ± 0.6 vs. 1.4 ± 1.2 ; $P = 0.3$), but these results did not reach significance. Figure 3 shows a schematic representation of the differentially expressed molecules and their functions.

To gain further insight into the role of these 375 differentially expressed genes, we performed a pathway analysis using Ingenuity Pathway Analysis Systems and identified 31 significantly differentially regulated pathways (some of which are listed in Table 3). The first few differentially regulated pathways were related to liver disease or injury, including: 1) liver X receptor/retinoid X receptor activation pathways, which play a major role in hepatic lipid synthesis; 2) hepatic cholestasis, a metabolic disease resulting from abnormal bile flow; 3) bile acid biosynthesis; 4) xenobiotic detoxification by cytochrome P450 enzymes; and 5) hepatic fibrosis and hepatic stellate cell activation. Of note, molecules found in these various pathways included *MMP9*; lipopolysaccharide binding protein; *CD14*, IL-1-receptor-antagonist; TNF receptor superfamily, member 11b; and *MCPI1*, which all belong to the nuclear factor- κ B (NF- κ B) signaling pathway.

DISCUSSION

Obesity is associated with inflammation, which may play an important role in fatty liver disease and insulin resistance (1,2,17,18). In this study, we showed that in a group of obese Hispanics and African Americans, 44% of the participants had adipose tissue inflammation, which was associated with higher amounts of VAT and liver fat, hyperinsulinemia, and reduced β -cell function. At the molecular level, individuals with CLS showed upregulation of several genes belonging to the NF- κ B stress pathway.

In obese individuals, inflammatory processes are thought to originate from the excessive accumulation of fat in the adipose tissue, where it translates into recruitment of macrophages around dead adipocytes, forming ring patterns known as CLS (12). Consistent with a role for CLS in adipose tissue inflammation, we demonstrated the presence of a subclass of proinflammatory macrophages, CD11c+ dendritic cells, which have been linked to systemic insulin resistance, only in adipose tissue of subjects with CLS (10,16). Moreover, we demonstrated that in obese Hispanics and African Americans, VAT, liver fat, and circulating TNF- α were significantly higher in individuals with CLS in fat biopsies, independent of ethnicity, sex, total body fat, and SAT. Such accumulation of fat in the visceral compartment and the liver markedly increases the risk for type 2 diabetes, and these metabolic abnormalities have been recognized as independent features of the metabolic syndrome (19,20). Indeed, inflammation is also closely associated with insulin resistance, both in the liver and the adipose tissue (21–23). This may be because of decreased insulin signaling by inflammatory mediators such as IL-1 and TNF- α (24). Consistent with these previous observations, we show that individuals with CLS (CLS+) had increased fasting glucose and insulin, as well as decreased DI, reflecting altered glucose homeostasis and β -cell function.

We further investigated the effect of inflammation separately in Hispanics and African Americans. The prevalence of individuals with inflammation was equally distributed among ethnicities, suggesting that there is no

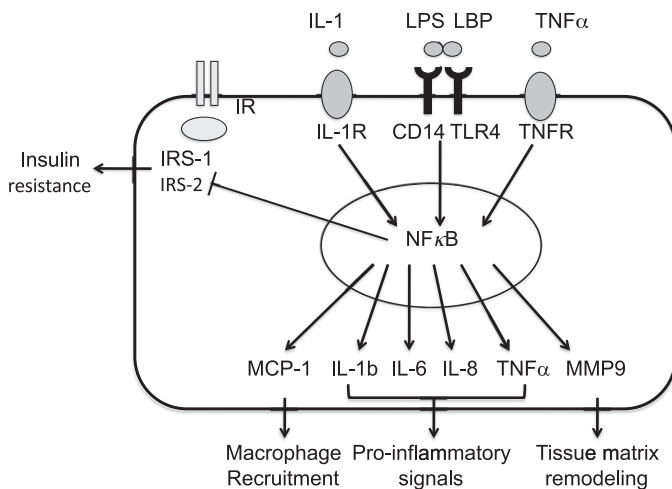


FIG. 3. In individuals with high macrophage aggregation around dead adipocytes as CLS, activation stimuli such as IL-1, lipopolysaccharide (LPS) and lipopolysaccharide binding protein (LBP), and TNF- α bind to their appropriate membrane receptors. Transduction of signal from receptors activates the NF- κ B pathway, which results in transcription of several secreted molecules and downregulates insulin signaling. In adipocytes, MCP-1 recruits macrophages and MMP9 stimulates adipocyte enlargement, whereas secreted ILs and TNF- α further activate inflammatory cascades and participate to insulin resistance development. TLR, Toll-like receptor; TNFR, TNF receptor.

existing ethnic predisposition to adipose tissue inflammation. Previous reports have shown that Hispanics are more prone to accumulation of lipids in the VAT and the liver (11). Given the tight link between ectopic fat and inflammation, we therefore expected Hispanics to have a higher degree of inflammation. However, our results show that inflammation may occur in Hispanics regardless of VAT amount. Moreover, presence of CLS was associated with lower SI and increased plasma TNF- α concentrations. In contrast, African Americans usually display lower amounts of VAT; in this ethnic group, we found that VAT was significantly increased only by the presence of adipose tissue inflammation. Although we cannot establish any causal relationship at this point, these ethnic discrepancies suggest that in Hispanics, presence of inflammation is not a major player in these adipose tissue depots accumulation, but is instead associated with the development of systemic inflammation and insulin resistance. By contrast, in African Americans, who are usually protected against VAT accumulation, presence of adipose tissue inflammation may reflect a generalized increase in adipocyte depot mass and activation of inflammatory pathways. This suggests that presence of adipose tissue inflammation may be linked to distinct metabolic outcomes, depending on ethnicity.

Based on these clinical observations, we investigated how different gene expression patterns between CLS+ and CLS- individuals could provide a functional link between adipose tissue inflammation, hepatic fat accumulation, and insulin resistance. As a result, several molecules related to the NF- κ B pathway were upregulated in CLS+ individuals. NF- κ B pathway mediates important stress responses and activates several proinflammatory cascades (25). Classically, its activation requires the binding of proinflammatory stimuli such as TNF- α , IL-1, or bacterial lipopolysaccharide to their appropriate membrane receptors, which subsequently trigger the activation cascade (26). Activation of NF- κ B results in enhanced transcription of IL-6, IL-8, and TNF- α , which trigger stress and inflammatory pathways and further

stimulate the NF- κ B pathway (21). NF- κ B also leads to increased MCP-1, which locally recruits macrophages, and MMP9, which plays a role in inflammation-mediated tissue remodeling, such as adipocyte size expansion (27) and fibrosis in the liver (28). Notably, all of these molecules were upregulated in CLS+ individuals in the current study, reflecting a higher degree of inflammation and macrophage activation (Fig. 3). In mononuclear cells from obese individuals, the NF- κ B pathway is also activated, contributing to higher blood concentrations of proinflammatory mediators such IL-6, TNF- α , and MMP9 (29). This suggests that CLS-associated macrophages may have similar roles in adipose tissue, thus contributing to local release of proinflammatory cytokines (27). Using pathway analysis, we also observed that the most differentially regulated pathways were related to liver functions/diseases, such as liver X receptor/retinoid X receptor activation, hepatic cholestasis, and hepatic fibrosis pathways, with activation of several genes related to inflammatory processes, and more specifically to the NF- κ B pathway. These pathways play pivotal roles in liver injury and may lead to increased hepatic lipid synthesis (30–32).

Our present results show that CLS may be found in some but not all obese individuals, independently of their ethnic background or sex, and is associated with increased VAT, hepatic fat content, and insulin resistance (33). Although our results are based on associations, when evaluated together with existing literature, the findings collectively suggest that with increasing obesity, adipocytes enlarge, until reaching a threshold (33). This may promote adipocyte death, macrophage aggregation, and CLS formation (8). The ensuing inflammatory activity may trigger the NF- κ B stress pathway and additional remodeling mechanism, characterized by increased MMP9 protease expression (34,35). Excess TG accumulation in adipose tissue may subsequently spill over to the systemic circulation and in turn accumulate in ectopic tissues, such as VAT and the liver (7,36), which may both contribute to decreased SI. The fact that in Hispanics high amounts of VAT are not necessarily associated with adipose tissue inflammation suggests that such relationships may be more subtle and possibly depend on other environmental and/or genetic factors.

One limitation of our study is the absence of nutritional data. Both high-fat or high-fructose diets induce insulin resistance and inflammation (37). It remains therefore possible that differences in dietary intakes may contribute to the inflammatory status of adipose tissue. Whether the nutritional status may affect adipose tissue inflammation and the presence of CLS over the long run remains to be investigated. Moreover, this study was limited to African Americans and Hispanics, and obesity duration was not collected. It remains therefore to determine how the onset and duration of obesity may affect adipose tissue inflammation in these populations. Finally, we did not separate adipocytes from other cell types. Further studies using cell sorting will be required to discriminate the expression profile between cell types within the adipose tissue.

In conclusion, this study demonstrates that macrophage infiltration in SAT from obese individuals is equally distributed between sexes and ethnicities. Presence of inflammation is associated with higher VAT and hepatic fat content, as well as higher fasting glucose and insulin and reduced β -cell function, independent of total fat. These phenotypes may be attributed to upregulation of major gene pathways involved in proinflammatory cascades, such as the NF- κ B stress pathway. Further intervention studies will be required to assess the time course of such metabolic alterations and establish causal

TABLE 3
Differentially regulated pathways between CLS+ and CLS− individuals

Canonical pathway	No. of genes	<i>P</i> value	Symbol
Liver X receptor/retinoid X receptor activation	9	4.20 E-05	CD14, CCL2, TNFRSF11B, APOC1, MSR1, MMP9, NGFR, IL1RN, LBP
Hepatic cholestasis	12	6.69 E-05	CD14, CYP27A1, ABCC3, SLCO3A1, TNFRSF11B, IRAK1, ESR1, NGFR, RARA, IL1RN, LBP, HSD3B7
Bile acid biosynthesis	7	9.26 E-05	CYP27A1, ALDH1A3, ADHFE1, DHRS9, ADH1A, ADH1B, HSD3B7
Metabolism of xenobiotics by cytochrome P450	10	1.17 E-04	AKR1C2, ALDH1A3, CYP2F1, ALDH3B2 (includes EG:222), ADHFE1, CYP2C9, CYP2S1, DHRS9, ADH1A, ADH1B
Atherosclerosis signaling	10	1.4 E-04	PDGFA, CXCR4, CCL2, ITGB2, ALOX5, MSR1, MMP9, PLA2G2A, TNFRSF12A, IL1RN
Hepatic fibrosis/hepatic stellate cell activation	11	2.7 E-04	CD14, PDGFA, TIMP1, CCL2, EDNRA, TNFRSF11B, AGTR1, MMP9, NGFR, EGFR, LBP
IL-10 signaling	7	6.6 E-04	CD14, FCGR2B, CCR1, IL1RN, LBP, FCGR2A, HMOX1
Fatty acid metabolism	9	9.4 E-04	ALDH1A3, CYP2F1, ADHFE1, AUH, CYP2C9, CYP2S1, DHRS9, ADH1A, ADH1B
Complement system	5	1.2 E-03	C5AR1, C1QC, C2, C3AR1, CFB
Fcγ receptor-mediated phagocytosis in macrophages and monocytes	8	1.71 E-03	LYN, FCGR1A, PLD3, FGR, SYK, FCGR2A, WAS, HMOX1
Lipopolysaccharide/IL-1-mediated inhibition of retinoid X receptor function	12	2.1 E-03	CD14, ABCC3, IL4I1, TNFRSF11B, ALDH1A3, APOC1, IRAK1, ALDH3B2 (includes EG:222), CYP2C9, NGFR, RARA, LBP
Acute phase response signaling	11	2.8 E-03	TNFRSF11B, IRAK1, SERPINA3, C2, NGFR, HAMP, IL1RN, HP, LBP, HMOX1, CFB
Dendritic cell maturation	10	2.9 E-03	FCGR2B, CD86, TNFRSF11B, TYROBP, FCGR1A, NGFR, IL1RN, TREM2, FCGR2A, FCGR1B
IL-9 signaling	4	6.8 E-03	IRS1, BCL3, IRS2, CISH
PPAR signaling	5	1.5 E-02	PDGFA, TNFRSF11B, CITED2, NGFR, IL1RN, PPARGC1A
IL-8 signaling	9	2.01 E-02	ITGB2, ITGAX, IRAK1, MMP9, PLD3, GNAI1, ANGPT2, EGFR, HMOX1
IL-6 signaling	6	2.07 E-02	CD14, TNFRSF11B, NGFR, IL1RN, LBP, TNFAIP6
Role of macrophages, fibroblasts, and endothelial cells in rheumatoid arthritis	13	3.6 E-02	PDGFA, F2RL1, TNFRSF11B, FCGR1A, CFB, C5AR1, CCL2, FZD2, IRAK1, NGFR, HP, IL1RN, TNFSF13B
Type 2 diabetes signaling	1.26E00	3.8E-02	IRS1, TNFRSF11B, IRS2, PKM2, NGFR, SMPD1

PPAR, peroxisome proliferator-activated receptor.

relationship between adipose tissue inflammation, hepatic fat accumulation, and development of insulin resistance.

ACKNOWLEDGMENTS

This work was supported by grants from the American Diabetes Association; National Institutes of Health Grant R01-DK-082574 to A.S.G.; the Robert C. and Veronica Atkins Foundation Grant to A.S.G. and M.I.G.; and the U.S. Department of Agriculture, Agricultural Research Service, under agreement No. 58-1950-7-70 to A.S.G. K.-A.L. is supported by a grant from the Swiss National Science Foundation (PBLA33-122719).

No potential conflicts of interest relevant to this article were reported.

K.-A.L. designed the study, contributed to data and sample collection, analyzed data, wrote the manuscript, and reviewed and edited the manuscript. S.M. analyzed data and reviewed and edited the manuscript. T.L.A., R.E.H., and T.C.A. contributed to data and sample collection and reviewed

and edited the manuscript. J.S.K. reviewed and edited the manuscript. E.B., C.X., and A.S.G. contributed to data and sample collection and reviewed and edited the manuscript. H.A. designed the study and reviewed and edited the manuscript. M.I.G. designed the study, analyzed data, and reviewed and edited the manuscript.

REFERENCES

- Olefsky JM, Glass CK. Macrophages, inflammation, and insulin resistance. *Annu Rev Physiol* 2010;72:219–246
- Kolak M, Westerbacka J, Velagapudi VR, et al. Adipose tissue inflammation and increased ceramide content characterize subjects with high liver fat content independent of obesity. *Diabetes* 2007;56:1960–1968
- Apovian CM, Bigornia S, Mott M, et al. Adipose macrophage infiltration is associated with insulin resistance and vascular endothelial dysfunction in obese subjects. *Arterioscler Thromb Vasc Biol* 2008;28:1654–1659
- Stefan N, Kantartzis K, Machann J, et al. Identification and characterization of metabolically benign obesity in humans. *Arch Intern Med* 2008;168:1609–1616
- Karelis AD, Faraj M, Bastard JP, et al. The metabolically healthy but obese individual presents a favorable inflammation profile. *J Clin Endocrinol Metab* 2005;90:4145–4150

6. Scherer PE. Adipose tissue: from lipid storage compartment to endocrine organ. *Diabetes* 2006;55:1537–1545
7. Savage DB, Petersen KF, Shulman GI. Disordered lipid metabolism and the pathogenesis of insulin resistance. *Physiol Rev* 2007;87:507–520
8. Cinti S, Mitchell G, Barbatelli G, et al. Adipocyte death defines macrophage localization and function in adipose tissue of obese mice and humans. *J Lipid Res* 2005;46:2347–2355
9. Shaul ME, Bennett G, Strissel KJ, Greenberg AS, Obin MS. Dynamic, M2-like remodeling phenotypes of CD11c+ adipose tissue macrophages during high-fat diet-induced obesity in mice. *Diabetes* 2010;59:1171–1181
10. Wentworth JM, Naselli G, Brown WA, et al. Pro-inflammatory CD11c+ CD206+ adipose tissue macrophages are associated with insulin resistance in human obesity. *Diabetes* 2010;59:1648–1656
11. Liska D, Dufour S, Zern TL, et al. Interethnic differences in muscle, liver and abdominal fat partitioning in obese adolescents. *PLoS ONE* 2007;2:e569
12. Weisberg SP, McCann D, Desai M, Rosenbaum M, Leibel RL, Ferrante AW Jr. Obesity is associated with macrophage accumulation in adipose tissue. *J Clin Invest* 2003;112:1796–1808
13. Hussain HK, Chenevert TL, Lundy FJ, et al. Hepatic fat fraction: MR imaging for quantitative measurement and display—early experience. *Radiology* 2005;237:1048–1055
14. Tumor Analysis Best Practices Working Group. Expression profiling—best practices for data generation and interpretation in clinical trials. *Nat Rev Genet* 2004;5:229–237
15. Cutfield WS, Bergman RN, Menon RK, Sperling MA. The modified minimal model: application to measurement of insulin sensitivity in children. *J Clin Endocrinol Metab* 1990;70:1644–1650
16. Patsouris D, Li PP, Thapar D, Chapman J, Olefsky JM, Neels JG. Ablation of CD11c-positive cells normalizes insulin sensitivity in obese insulin resistant animals. *Cell Metab* 2008;8:301–309
17. Harman-Boehm I, Blüher M, Redel H, et al. Macrophage infiltration into omental versus subcutaneous fat across different populations: effect of regional adiposity and the comorbidities of obesity. *J Clin Endocrinol Metab* 2007;92:2240–2247
18. Xu H, Barnes GT, Yang Q, et al. Chronic inflammation in fat plays a crucial role in the development of obesity-related insulin resistance. *J Clin Invest* 2003;112:1821–1830
19. Gastaldelli A, Miyazaki Y, Pettiti M, et al. Metabolic effects of visceral fat accumulation in type 2 diabetes. *J Clin Endocrinol Metab* 2002;87:5098–5103
20. Machado M, Cortez-Pinto H. Non-alcoholic steatohepatitis and metabolic syndrome. *Curr Opin Clin Nutr Metab Care* 2006;9:637–642
21. Cai D, Yuan M, Frantz DF, et al. Local and systemic insulin resistance resulting from hepatic activation of IKK-beta and NF-kappaB. *Nat Med* 2005;11:183–190
22. Mehta NN, McGillicuddy FC, Anderson PD, et al. Experimental endotoxemia induces adipose inflammation and insulin resistance in humans. *Diabetes* 2010;59:172–181
23. Ghanim H, Aljada A, Daoud N, Deopurkar R, Chaudhuri A, Dandona P. Role of inflammatory mediators in the suppression of insulin receptor phosphorylation in circulating mononuclear cells of obese subjects. *Diabetologia* 2007;50:278–285
24. Tanti JF, Jager J. Cellular mechanisms of insulin resistance: role of stress-regulated serine kinases and insulin receptor substrates (IRS) serine phosphorylation. *Curr Opin Pharmacol* 2009;9:753–762
25. Ahn KS, Aggarwal BB. Transcription factor NF-kappaB: a sensor for smoke and stress signals. *Ann N Y Acad Sci* 2005;1056:218–233
26. Bonizzi G, Karin M. The two NF-kappaB activation pathways and their role in innate and adaptive immunity. *Trends Immunol* 2004;25:280–288
27. Nair S, Lee YH, Rousseau E, et al. Increased expression of inflammation-related genes in cultured preadipocytes/stromal vascular cells from obese compared with non-obese Pima Indians. *Diabetologia* 2005;48:1784–1788
28. Han YP, Yan C, Zhou L, Qin L, Tsukamoto H. A matrix metalloproteinase-9 activation cascade by hepatic stellate cells in trans-differentiation in the three-dimensional extracellular matrix. *J Biol Chem* 2007;282:12928–12939
29. Ghanim H, Aljada A, Hofmeyer D, Syed T, Mohanty P, Dandona P. Circulating mononuclear cells in the obese are in a proinflammatory state. *Circulation* 2004;110:1564–1571
30. Herrema H, Meissner M, van Dijk TH, et al. Bile salt sequestration induces hepatic de novo lipogenesis through farnesoid X receptor- and liver X receptor alpha-controlled metabolic pathways in mice. *Hepatology* 2010;51:806–816
31. Shimomura I, Bashmakov Y, Ikemoto S, Horton JD, Brown MS, Goldstein JL. Insulin selectively increases SREBP-1c mRNA in the livers of rats with streptozotocin-induced diabetes. *Proc Natl Acad Sci USA* 1999;96:13656–13661
32. Endo M, Masaki T, Seike M, Yoshimatsu H. TNF-alpha induces hepatic steatosis in mice by enhancing gene expression of sterol regulatory element binding protein-1c (SREBP-1c). *Exp Biol Med (Maywood)* 2007;232:614–621
33. Tchoukalova YD, Koutsari C, Karpak MV, Votruba SB, Wendland E, Jensen MD. Subcutaneous adipocyte size and body fat distribution. *Am J Clin Nutr* 2008;87:56–63
34. Unal R, Yao-Borengasser A, Varma V, et al. Matrix metalloproteinase-9 is increased in obese subjects and decreases in response to pioglitazone. *J Clin Endocrinol Metab* 2010;95:2993–3001
35. Bourlier V, Zakaroff-Girard A, Miranville A, et al. Remodeling phenotype of human subcutaneous adipose tissue macrophages. *Circulation* 2008;117:806–815
36. Duval C, Thissen U, Keshtkar S, et al. Adipose tissue dysfunction signals progression of hepatic steatosis towards nonalcoholic steatohepatitis in C57BL/6 mice. *Diabetes* 2010;59:3181–3191
37. Ghanim H, Abuaysheh S, Sia CL, et al. Increase in plasma endotoxin concentrations and the expression of toll-like receptors and suppressor of cytokine signaling-3 in mononuclear cells after a high-fat, high-carbohydrate meal: implications for insulin resistance. *Diabetes Care* 2009;32:2281–2287